CHAPTER 3

EXPERIMENTAL METHODS

In this work, two types of proton-conducting methyl cellulose (MC) polymer electrolytes have been prepared. The first system is unplasticized MC-NH_4NO_3 complexes; to study the effect of NH_4NO_3 salt in MC based polymer electrolyte and the other system is MC-NH_4NO_3 plasticized with PEG; to study the effect of PEG as a plasticizer.

3.1 Electrolyte preparation

Figure 3.1 depicts a pictorial flow chart for the procedure of electrolyte preparation.

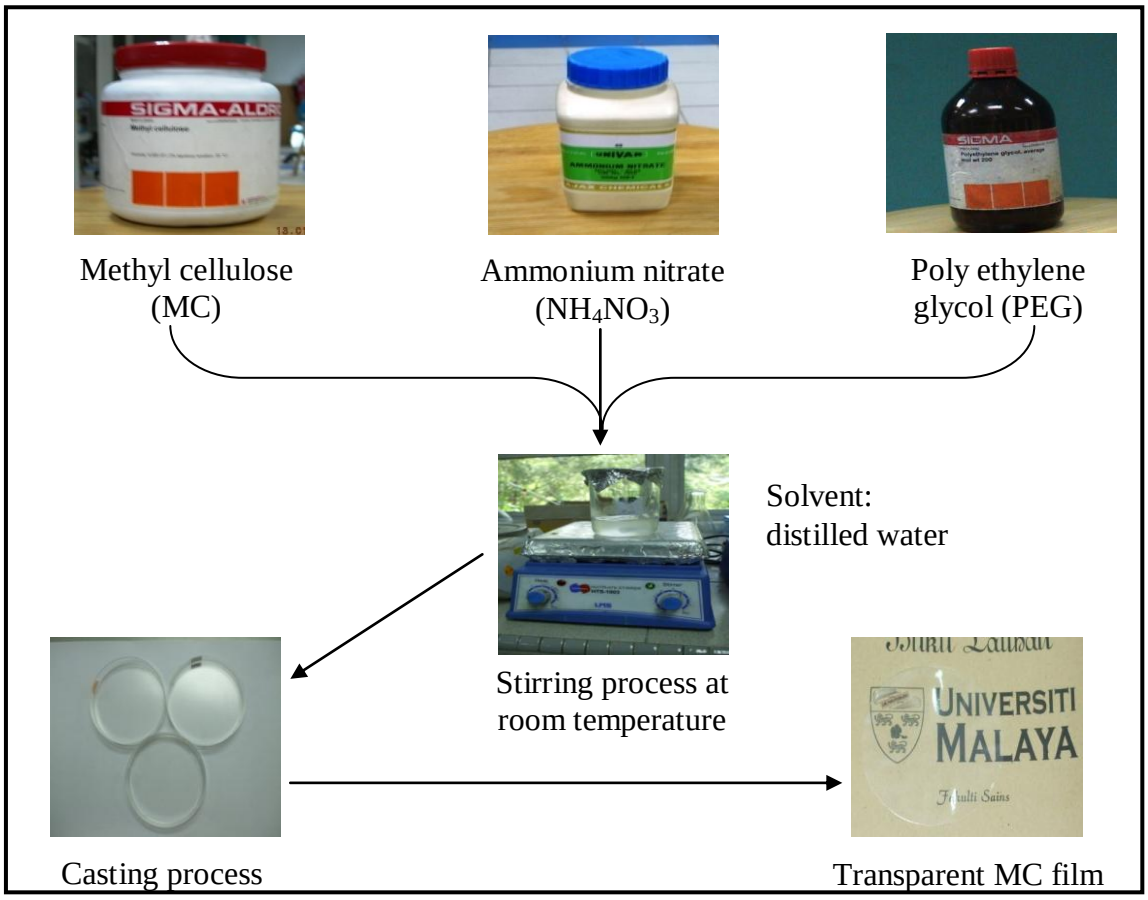

Figure 3.1: Flow chart of electrolyte preparation

3.1.1 Unplasticized MC: NH_4NO_3 complexes

The electrolyte films were prepared by the technique of solution casting. Table 3.1 lists the amounts of MC and NH_4NO_3 used to prepare the different electrolytes.

Table 3.1: The composition of MC doped NH_4NO_3

Sample Designation	MC (g)	NH_4NO_3 (g)	wt.% of NH_4NO_3
Pure MC	2	0.0000	0
95MC5AN	2	0.1053	5
90MC10AN	2	0.2222	10
85MC15AN	2	0.3529	15
80MC20AN	2	0.5000	20
75MC25AN	2	0.6667	25
70MC30AN	2	0.8571	30

MC purchased from Sigma-Aldrich has viscosity: 4000 cP (2 % aqueous solution, 20 ºC). NH_4NO_3 purchased from Ajax, was used as received. Distilled water was used as solvent. Water was used as a solvent because MC only dissolves in distilled water due to degree of substitution as discussed in Chapter Two. MC is a hydrophilic polymer. According to Hatakeyama and Hatakeyama (1998), polymers with hydrophilic groups such as hydroxyl groups have various strengths of interaction with water.

According to Table 3.1, 2 g of MC was dissolved in distilled heated at 50 ºC and stirred for a few hours to form a clear viscous solution. Desired amounts of NH_4NO_3

(purchased from Ajax) were added and stirred until complete dissolution of the salt. The mixtures were then cast into different Petri dishes and left to dry by evaporation at room temperature to form films. The films were kept in a dry box to ensure dryness of the film with RH ~ 30 %. Usually, polymer-salted electrolytes give low conductivity, less than 10^{-4} S cm^{-1} at room temperature [Kato *et al*., 2002]. This is insufficient for practical applications in electrochemical devices.

3.1.2 Plasticized MC-NH_4NO_3 system with PEG

Awadhia and Agrawal (2007) pointed that, in the crystalline phase, polymer electrolytes has poor conductivity. Ionic conduction occurs mainly in the amorphous phase. High conducting polymer electrolyte (PE) is very important for application in electrochemical devices. To enhance the conductivity of PE, plasticizers such as ethylene carbonate (EC), polycarbonate (PC), dimethyl sulfoxide (DMSO), polypropylene glycol (PPG), polyethylene glycol (PEG) and ethylene sulfate (ES) can be added to the PE solution.

The plasticizer should have low viscosity and high dielectric constant [Pradhan *et al*., 2009]. The low viscosity will help to decrease the glass transition temperature, T_g and increase the amorphous content. The high dielectric constant of the plasticizer helps to dissociate the salt or ion aggregates.

In this work, low molecular weight PEG (200) was chosen as a plasticizer due to its non-volatility, non-toxicity, biodegradability, and low price making it a promising green solvent for different purposes [Hou *et al*., 2007; Naik & Doraiswamy, 1998; Chen *et al*.,

2004; Leininger *et al*., 2004]. Park and Ruckestein (2001) pointed that, among the many plasticizers, PEG is most suitable for MC in the preparation of PEs because PEG is sufficiently hygroscopic enabling it to retain moderate moisture in the polymer and improves its flexibility without decreasing its mechanical strength.

Table 3.2 below shows the amounts of MC, NH_4NO_3 salt and PEG used in the preparation of plasticized polymer electrolyte samples.

Table 3.2: The composition of plasticized polymer electrolytes prepared

Sample Designation	**MC (g)**	**NH_4NO_3 (g)**	**PEG (ml)**	**wt.% of PEG**
75.00MC25.00AN0PEG	2	0.6667	0	0
71.25MC23.75AN5PEG	2	0.6667	0.1582	5
67.50MC22.50AN10PEG	2	0.6667	0.2963	10
63.75MC21.25AN15PEG	2	0.6667	0.5304	15
80.00MC20.00AN20PEG	2	0.6667	0.7513	20
56.25MC18.75AN25PEG	2	0.6667	1.0018	25

The highest conducting polymer-salt film obtained from the polymer-salt system contains 25 wt.% of NH_4NO_3. To this, different amounts of polyethylene glycol (PEG 200) were added. The solution was poured into Petri dishes and left to dry by evaporation at room temperature for films to form. The films were kept in a dry box to prevent absorption of moisture.

Figure 3.2 displays the flow chart for the experimental work on electrolyte.

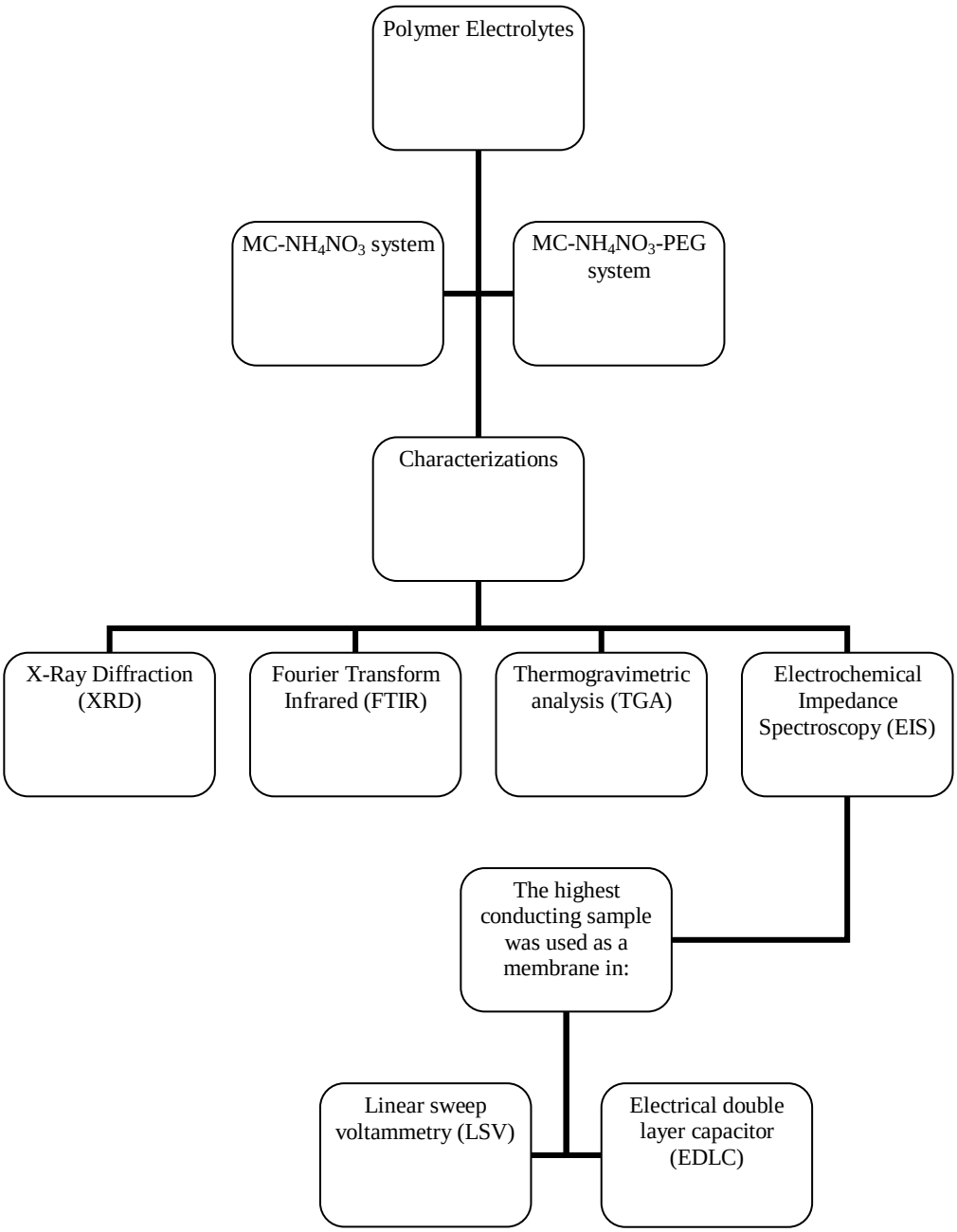

Figure 3.2: Flow chart of experimental work

3.2 X-ray diffraction (XRD)

Figure 3.3: XRD machine

The nature of the films was studied by XRD technique using the Siemens D5000 X-ray diffractometer as shown in Figure 3.3 from 2θ angles between 5º and 80º. The wavelength of the monochromatic Cu Kα radiation is 1.5406 Å. The operating current was 40 mA and operating voltage, 40 kV. Step size for MC-NH_4NO_3 system was 0.1º and for plasticized MC-NH_4NO_3 system was 0.05º.

Figure 3.4 shows examples of x-ray diffractrogams for pectin based gel electrolyte. Normally, a polymer is semi-crystalline. Crystalline materials have ordered molecular structure with sharp melting points while amorphous materials have randomly ordered structure. According to Figure 3.4, pectin powder (a natural polymer) is semi-crystalline with several sharp peaks. After addition of plasticizer, the samples show amorphous

characteristics that is, a broad diffuse bands centered at 2θ = 21º with a small shoulder at 2θ = 9º for the sample containing 37 wt.% glycerol [Andrade *et al.*, 2009].

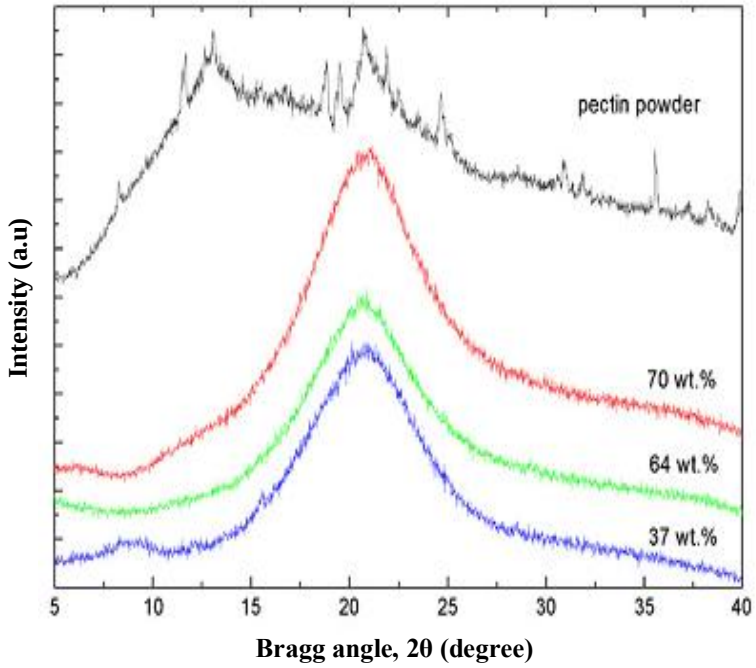

Figure 3.4: X-ray diffraction for pectin based gel electrolyte containing various wt. % of glycerol (Andrade *et al.*, 2009)

3.3 Fourier transforms infrared spectroscopy (FTIR)

In this work, FTIR spectrometer as shown in Figure 3.5 was used to determine the position of functional groups in MC and to determine the shift in these functional groups (if any) as a result of complexation (or interaction) between lone pair electrons in donor atoms. According to Selvasekarapandian *et al*. (2006) FTIR spectroscopy can be used to study the interactions between ions or atoms in a polymer electrolyte. These interactions can induce changes in the vibrational modes of the molecules in the polymer electrolytes.

Figure 3.5: FTIR machine

Examples of FTIR spectrum for polymer electrolyte systems are shown in Figure 3.6.

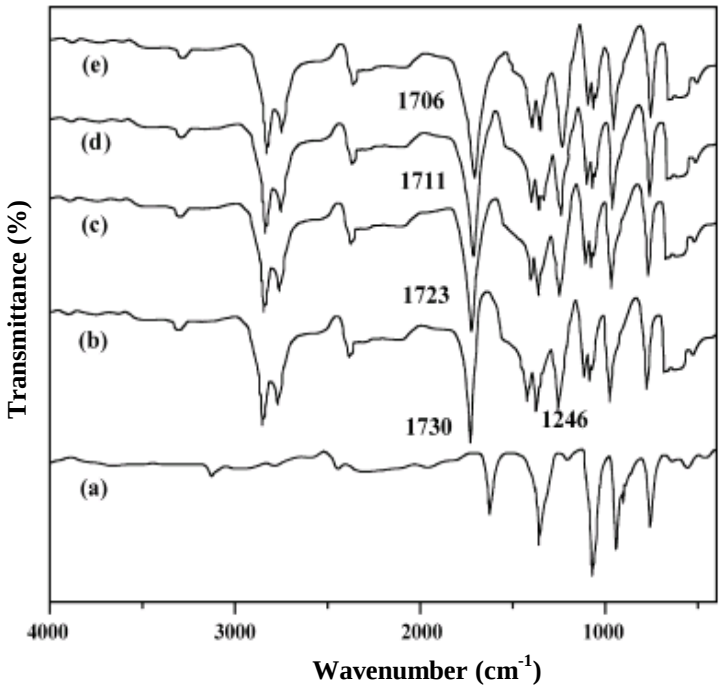

Figure 3.6: FTIR spectra for (a) pure $LiClO_4$, (b) pure PVAc, (c) 90PVAc:10$LiClO_4$, (d) 85PVAc:15$LiClO_4$, (e) 80PVAc:20$LiClO_4$ (Selvasekarapandian *et al.*, 2006)

Selvasekarapandian *et al*. (2006) studied the interaction in PVAc-$LiClO_4$ polymer-salt complex and found that the lithium ion "binds" with the polymer. As depicted in Figure

3.6, the vibrational bands of CH_3 asymmetric stretching , symmetric stretching and symmetric bending vibrations of pure PVAc was observed at 2923, 2865 and 1375 cm^{-1}, respectively. The peaks attributable to C-O-C symmetrical stretching, C-O and C-C stretching were observed at 1245, 1100 and 1090 cm^{-1}, respectively. The interaction in polymer electrolytes can be observed by shifting the vibrational bands of PVAc from 2923, 1375, 1090 and 940 cm^{-1} to 2932, 1372, 1085 and 930 cm^{-1} and vibrational bands of $LiClO_4$ from 940 cm^{-1} to 942-963 cm^{-1}. The appearance of strong band in the spectrum at 1730cm^{-1} which correspond to C=O stretching frequency of pure PVAc is broadened and shifted to lower wavenumbers at 1730-1706 cm^{-1} with increase in concentration of $LiClO_4$ as shown in Table 3.3.

Table 3.3: FTIR modes of ester oxygens in PVAc-$LiClO_4$ polymer electrolytes (Selvasekarapandian *et al*., 2006)

PVAc-$LiClO_4$ complexes	C=O band variations (cm^{-1})
Pure PVAc	1730
90:10	1723
85:15	1711
80:20	1706

In this work, infrared spectroscopy studies were performed using Thermo scientific/Nicolet iS10 spectrometer with the resolution of 1 cm^{-1}. The spectrum is taken from 650 cm^{-1} to 4000 cm^{-1}.

3.4 Thermogravimetric analysis (TGA)

TGA is a simple and accurate method for studying the decomposition pattern and the thermal stability of polymers [Zohuriaan and Shokrolahi, 2004]. Ramesh and Arof

(2001) studied the thermal characteristics of poly (vinyl chloride) based polymer electrolytes and found that the thermal stability of polymer electrolytes decreases with addition of plasticizers. Examples of thermogravimetric analysis are depicted in Figure 3.7.

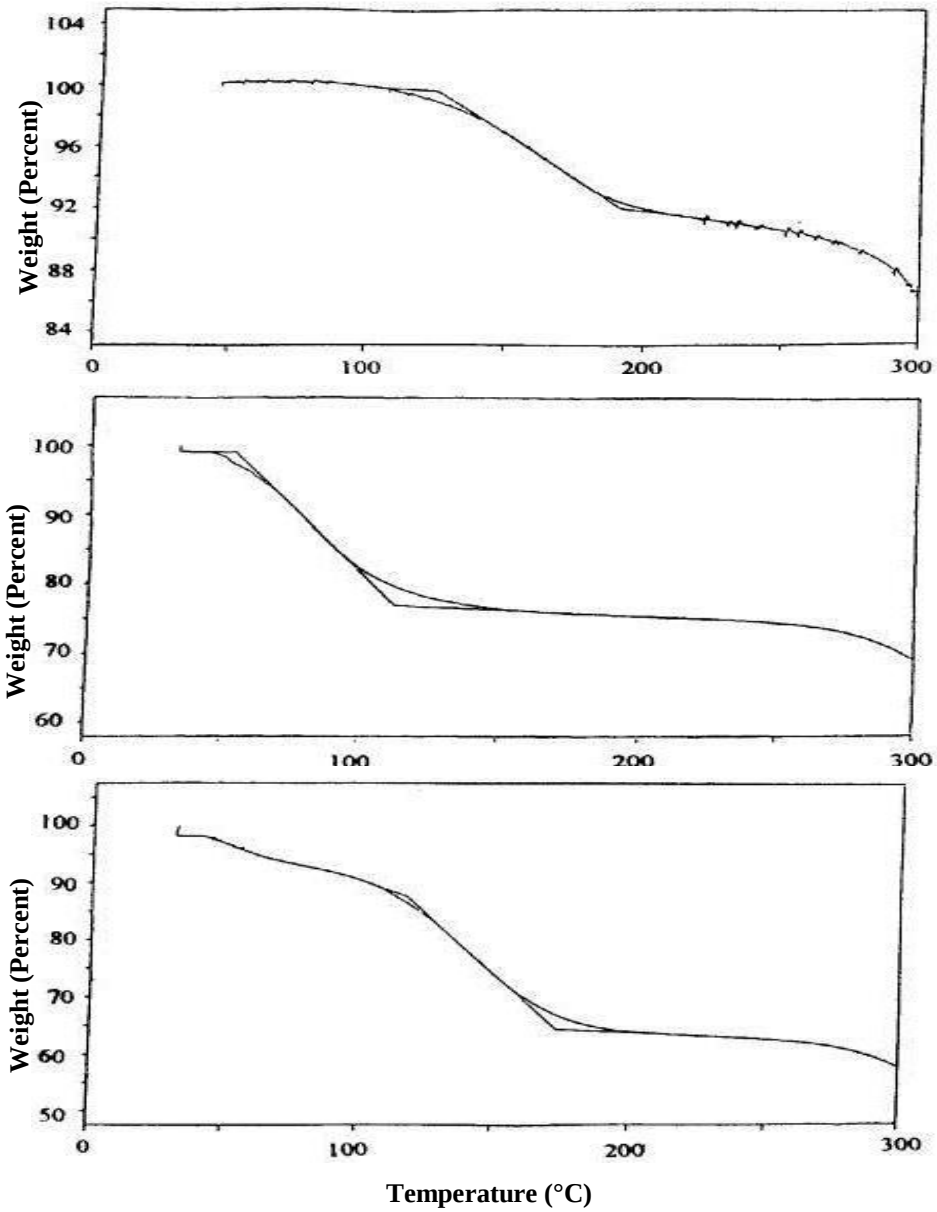

Figure 3.7: TGA thermograms of (a) pure PVC, (b) $0.7LiBF_4$+$0.3LiCF_3SO_3$+PVC, (c) PVC:$LiBF_4$:$LICF_3SO_3$:EC:PC (Ramesh and Arof, 2001)

For Figure 3.7 (a), the pure PVC film seems quite dry since its weight is almost constant up to 100 ºC. For polymer-salt system, the TGA curve of the $0.7LiBF_4$ +

$0.3LiCF_3SO_3$ + PVC is depicted in Figure 3.7 (b). The sample starts to lose mass at temperatures below 100 ºC with weight loss percentage of ~ 24 %. This is due to residual solvent evaporation and free water loss**.** The second weight loss begins at temperatures of above 250 ºC, due to crystallization of the sample. Figure 3.7 (c) shows the TGA curve for double plasticizer PVC: $LiCF_3SO_3$: $LiBF_4$: EC: PC complex. The curve shows weight loss of 7 % at temperatures below 100 ºC and 28 % at around 150 ºC. The second weight loss is due to crystallization of the samples. From TGA analysis, the decrease in crystallization temperature when plasticizer was added can be observed.

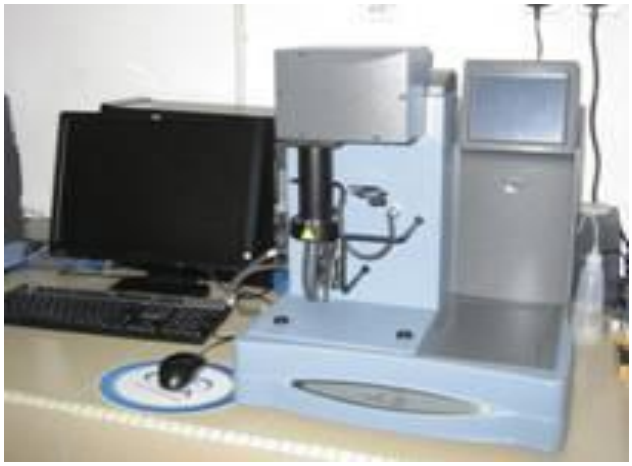

Figure 3.8: TGA machine

Thermal analysis of MC based polymer electrolytes was carried out using thermogravimetric analyzer as shown in Figure 3.8. The test was performed with a TGA Q500 (Instrument serial number: Q500-1448) and software version TA Universal Analysis. The measurements were carried out from 30 to 580 ºC at a heating rate of 30 ºC min^{-1} under nitrogen flow of 60 mL min^{-1} and air 40 mL min^{-1}. Mass of samples used for TGA measurements is around 4.40 to 4.95 mg.

3.5 Electrochemical impedance spectroscopy (EIS)

The impedance of the polymer electrolytes were measured using the HIOKI 3531-01 LCR bridge as shown in Figure 3.9 in the frequency range from 50 Hz to 1 MHz between temperatures 298 to 373 K. The thickness of each sample was measured using a micrometer screw gauge and the samples were cut into a suitable size and sandwiched between blocking stainless steel electrodes with diameter 2 cm.

Figure 3.9: EIS measurement

3.5.1 Conductivity measurements

The conductivity, σ was determined following the equation below:

$$\sigma = \frac{d}{R_b A} \tag{3.1}$$

where d and A is the thickness and area of the sample respectively and R_b is bulk resistance obtained from the Cole-Cole plot, $-Z_i$ versus Z_r as shown in Figure 3.10. Figure 3.10 (a) depicts the examples of Cole-Cole plot for pure PVA-chitosan blend and shows a tilted semicircle implying that the material is partially resistive and capacitive. Figure 3.10 (b)

and (c) shows the Cole-Cole plot for highest conducting sample for polymer-salted system and plasticized polymer electrolytes system respectively. The samples with salt and containing both salt and plasticizer are very capacitive in nature. The bulk resistance was obtained from intercept of the plot with the real axis.

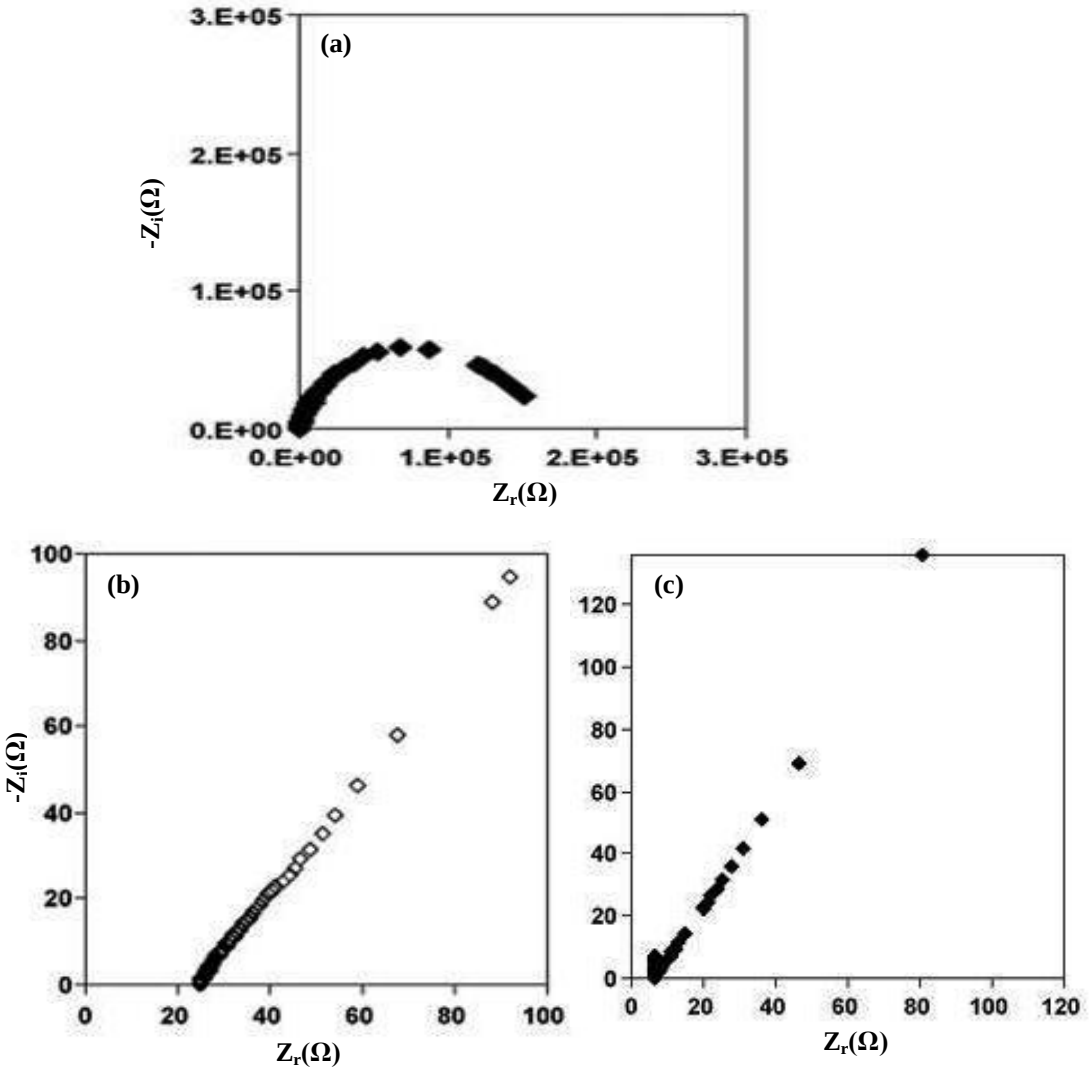

Figure 3.10: Cole-Cole plot for (a) PVA-chitosan blend, (b) PVA-chitosan-40 wt.% NH_4NO_3, (c) PVA-chitosan-40 wt.% NH_4NO_3-70 wt.% EC at room temperature (Kadir *et al*., 2010)

3.5.2 Dielectric characteristics

Dielectric calculations reveal significant information about the chemical and physical state of polymers. These properties such as dielectric constant and dielectric loss are drastically affected by the presence of another polymer or a dopant in the polymer [Rao *et al.*, 2000]. Dielectric constant plays a fundamental role which shows the ability of a polymer material to dissolve salts [Singh and Gupta, 1998]. The real and imaginary parts of complex dielectric constant and modulus were calculated using the equations below:

The real part of complex dielectric constant:

$$\varepsilon_r = \frac{Z_i}{\omega C_0 \left(Z_r^{\,2} + Z_i^{\,2}\right)} \tag{3.2}$$

The imaginary part of complex dielectric constant:

$$\varepsilon_i = \frac{Z_r}{\omega C_0 \left(Z_r^{\,2} + Z_i^{\,2}\right)} \tag{3.3}$$

where $C_0 = \varepsilon_o \frac{A}{t}$, ε_0 is the permittivity of the free space and $\omega = 2\pi f$ where f being the frequency in Hz. ε_r and ε_i are related to the capacitive and conductive nature of the material [Núñez *et al.*, 2004].

The real part of modulus, M_r is given by

$$M_r = \frac{\varepsilon_r}{\left(\varepsilon_r^{\,2} + \varepsilon_i^{\,2}\right)} \tag{3.4}$$

The imaginary part of modulus, M_i is given by

$$M_i = \frac{\varepsilon_i}{(\varepsilon_r^{\,2} + \varepsilon_i^{\,2})} \tag{3.5}$$

The loss tangent, tan δ is defined as:

$$\tan\delta = \frac{\varepsilon_i}{\varepsilon_r} = \frac{M_i}{M_r} \tag{3.6}$$

Figures 3.11 and 3.12 show respectively the variations of dielectric constant, ε_r and tan δ of polymer nanocomposite electrolytes with frequency for different concentrations of PEG.

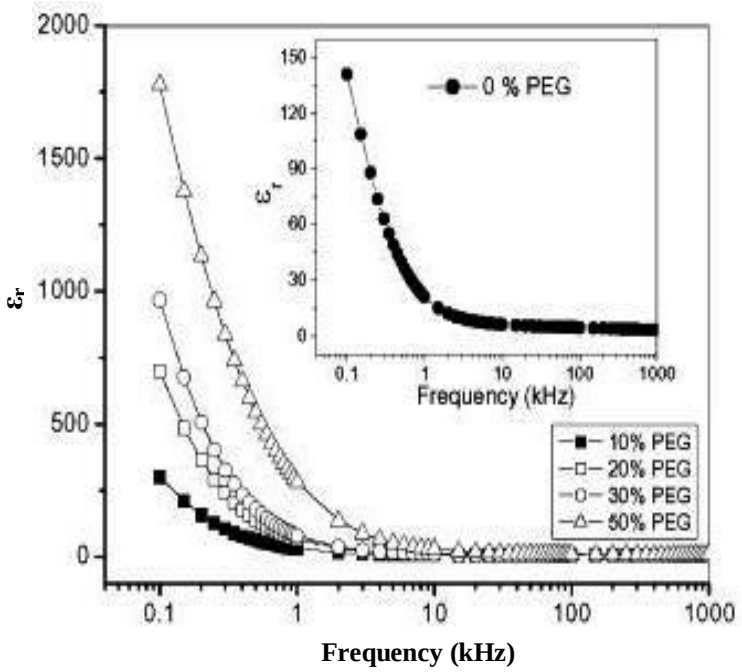

Figure 3.11: Variation of relative dielectric constant, ε_r of polymer nanocomposite electrolytes with frequency for different concentration of PEG at room temperature (Pradhan *et al.*, 2009).

At low frequency, the variation of dielectric constant with frequency shows the occurrence of polarization processes at the electrode/material interface. The loss tangent peaks appear at a characteristic frequency suggesting the presence of relaxing dipoles in all samples. The peaks shift towards higher frequency side with addition of plasticizer suggesting shortening of the relaxation time.

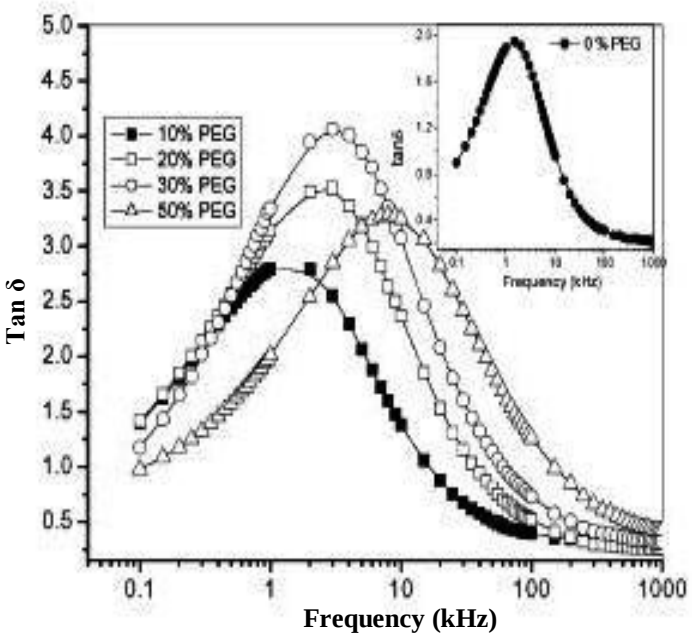

Figure 3.12: Variation of tan δ of polymer nanocomposite electrolytes with frequency for different concentration of PEG at room temperature (Pradhan *et al*., 2009).

3.5.3 Rice and Roth model

The Rice and Roth equation is based on the hypothesis that conducting ions can be thermally excited to propagate as free ions throughout the solid with velocity that is related to the activation energy, E_A. Using the Rice and Roth model, the number density of the mobile ions can be estimated using equation as shown below:

$$\sigma = \frac{(Ze)^2}{3kT} nvl \exp\left(-\frac{E_A}{kT}\right) \qquad (3.7)$$

Here Z =1 for proton charge carriers, E_A and m is the activation energy and mass of the proton respectively. k is Boltzmann constant and T is experimental temperature. l is the mean free path or distance between coordinating sites (electron donating atoms) and v is the velocity of the free ions was obtained by the equation $v=\left(\frac{2E_A}{m}\right)^{1/2}$. E_A can be obtained from the slope of the plot of log σ vs 1000/T. Yokota *et al*. (2007) pointed that the length of 40 rigid chain segments of bendable molecular cellulose is (60 ± 15) nm. From that, the length of one chain segment is 1.5 nm. So the value of l for MC used in the Rice and Roth equation is taken as 1.5 nm.

The ionic mobility is defined as:

$$\mu=\frac{\sigma}{nl} \tag{3.8}$$

and the diffusion coefficient is given by:

$$D=\frac{\sigma kT}{ne^2} \tag{3.9}$$

Table 3.4 lists some transport parameters reported by Majid and Arof (2005) obtained using equations shown above.

Table 3.4: Transport parameters of chitosan acetate complexes (Majid and Arof, 2005)

Sample	σ_{RT} (S cm^{-1}) × 10^{-9}	T (s) × 10^{-14}	μ (cm^2 v^{-1} s)	D (cm^2 s^{-1})	*E*a (eV)	*n* (cm^{-3}) × 10^{18}
E1	09.43	08.16	3.50×10^{-8}	9.00×10^{-10}	0.79	1.70
E2	43.40	08.38	8.00×10^{-8}	2.10×10^{-9}	0.74	3.40
E3	481.00	08.84	7.50×10^{-7}	1.90×10^{-8}	0.67	4.00
E4	6020.00	10.3 0	4.00×10^{-6}	1.00×10^{-7}	0.49	9.50
E5	25300.00	10.8 0	5.30×10^{-6}	1.40×10^{-7}	0.45	0.30
E6	3750.00	09.11	2.10×10^{-6}	5.50×10^{-8}	0.63	11.00

3.6 Linear sweep voltammetry (LSV)

Electrochemical stability window is a very important parameter required for the practical applications of batteries and capacitors. Electrochemical stability window of the polymer electrolyte was determined by linear sweep voltammetry using an AUTOLAB potentiostat/galvanostat at a 10 mV s^{-1} scan rate in the potential range from -2.5 to 2.5 V. The polymer electrolyte was sandwiched between a stainless steel that serves as the working electrode and MnO_2 as the counter and reference electrodes.

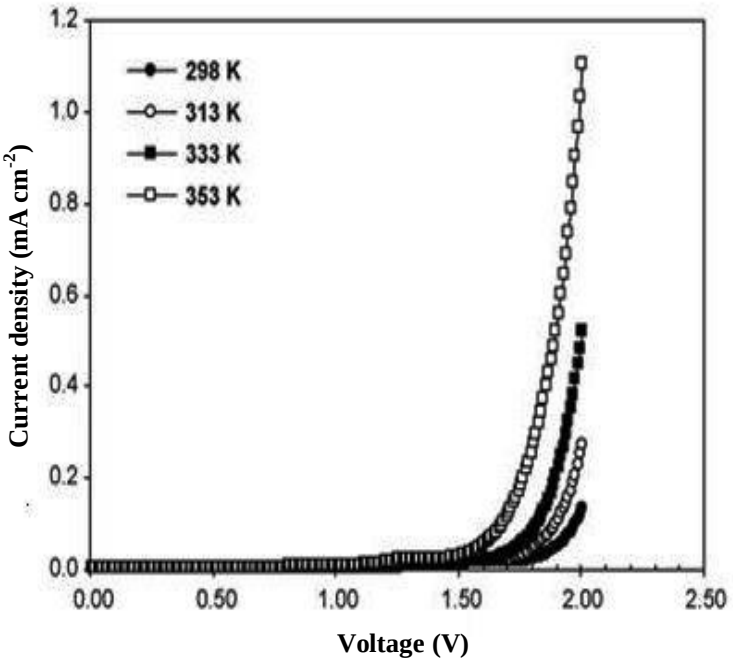

Figure 3.13 Linear sweep voltammetry (LSV) curves of sample 18 wt.% chitosan acetate + 12 wt.% NH_4NO_3 + 70 wt.% EC at 298, 313, 333 and 353 K (Ng and Mohamad, 2008) using stainless steel electrodes.

Figure 3.13 above shows the LSV curves for the sample 18 wt.% chitosan acetate + 12 wt.% NH_4NO_3 + 70 wt.% EC. It can be seen that, the sample has stable potential window with no appreciable current flow in the electrode up to 1.80, 1.75, 1.70 and 1.60 V

at temperatures of 298, 313, 333 and 353 K respectively. These voltages are high enough to allow safe use in the fabrication of proton batteries.

3.7 Electrical double layer capacitor (EDLC)

3.7.1 Electrode preparation

Figure 3.14 below shows the preparation procedure for the electrode part of EDLC.

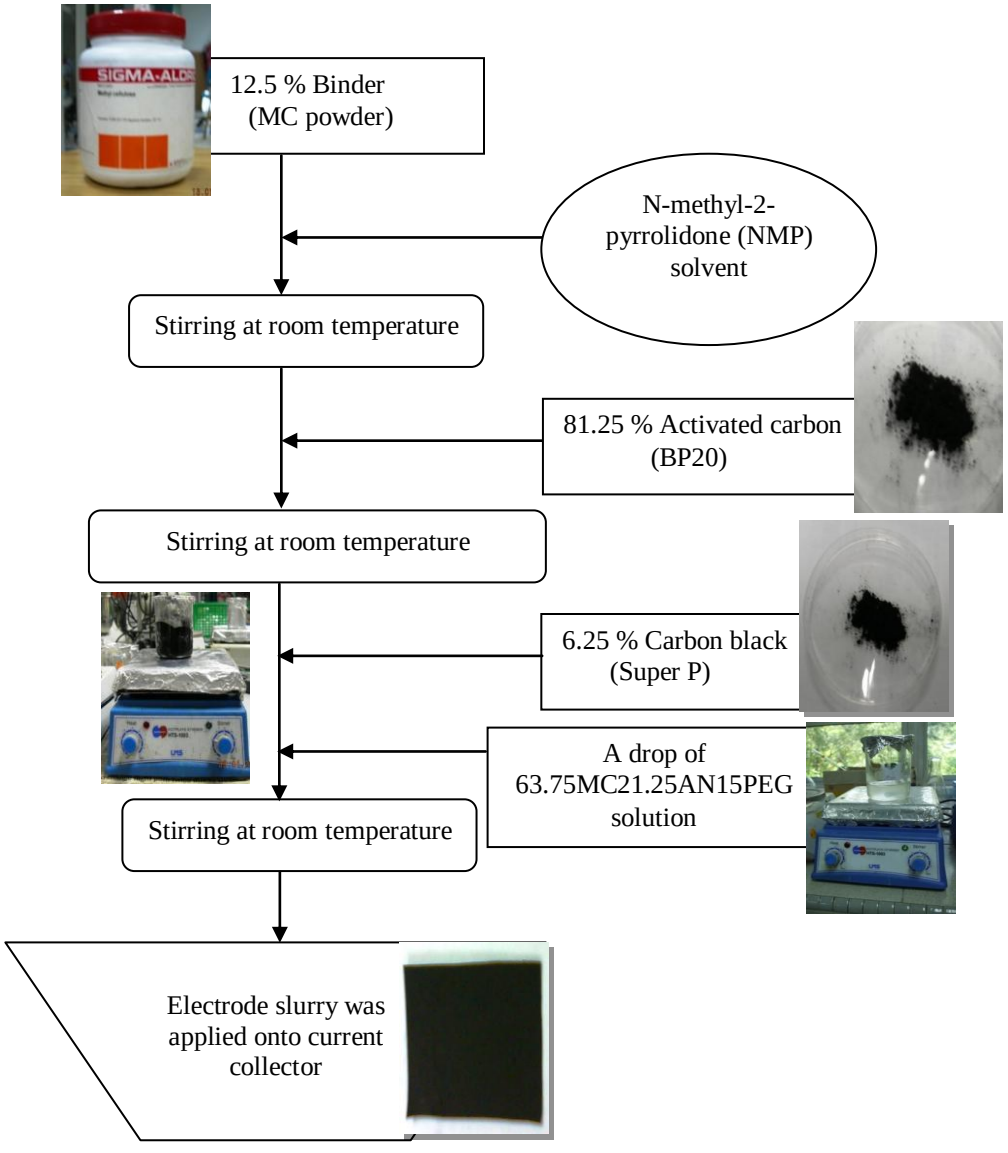

Figure 3.14 Preparation procedures for the electrode of EDLC

Methyl cellulose (MC) was stirred in N-methyl-2-pyrrolidone (NMP). Activated carbon (BP20, specific area = 1700 m^2 g^{-1} to 1800 m^2 g^{-1} purchased from Kuraray Chemical Co., LTD was added to the solution and stirred. Finally, carbon black (super P) were added and stirred for 24 H. The ratio of MC powder: activated carbon: carbon black is 0.8125:0.125:0.0625. The solution was then applied onto the current collector using dip coating method. Carbon black was added in the mixture of BP20-MC to enhance electron conduction.

3.7.2 EDLC fabrication

The EDLC was fabricated by sandwiching the polymer electrolytes between the electrodes. The EDLC was clamped between Perspex plates. The performance of all EDLCs fabricated was monitored using the AUTOLAB PGSTAT 12 potentiostat/galvanostat as shown in Figure 3.15.

Figure 3.15: AUTOLAB PGSTAT 12 potentiostat/galvanostat

3.8 EDLC characterization

Characterization of EDLC consists of:

a) Evaluation of specific capacitance as a function of charge/discharge rate employing cyclic voltammetry and constant current charging/discharging characteristics.

b) Examination of reversibility, efficiency, maximum energy and power delivered

Cyclic voltammetry and galvanostatic charge/discharge cycling were performed using Autolab PGSTAT 12 potentiostat/galvanostat. Cyclic voltammetry tests were conducted at scan rate 1 mV s^{-1} between 0 to 0.85 V in a two electrode configuration. Galvanostatic charging/discharging test were performed in the voltage range between 0 to 0.85 V at a constant current of 1 mA.

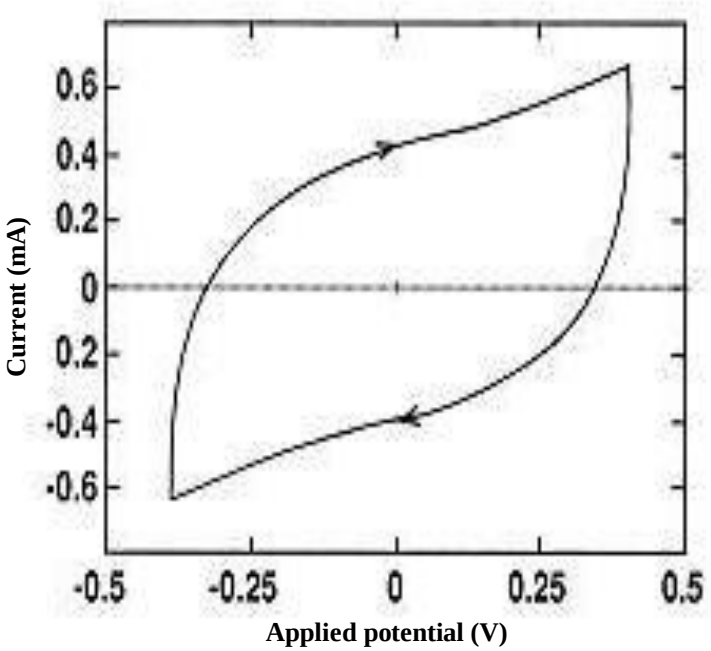

Figure 3.16 Cyclic voltammogram of a totally solid state electric double-layer capacitor fabricated. The measurement was carried out in an ambient atmosphere at room temperature under a sweep rate of 0.5 mV s^{-1} (Matsuda *et al.*, 1999)

Figure 3.16 shows cyclic voltammogram reported by Matsuda *et al*. (1999). This result shows no redox peak in a sweep region of 0.4 to -0.4 V and the capacitive current curve is smooth and varies from + 0.62 to – 0.62 mA. From the figure, electric charge stored in the electric double-layer at the interface between the polarizable electrodes can be deduced.

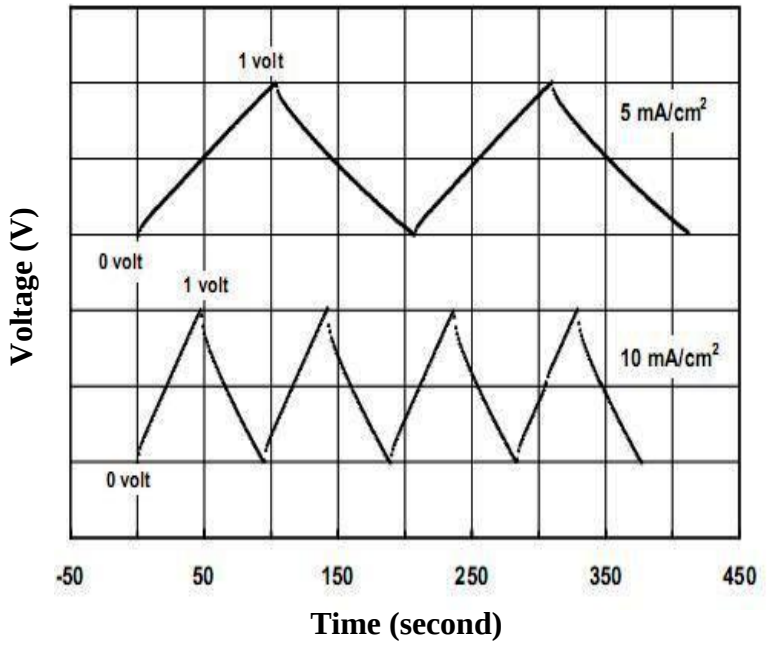

Figure 3.17 Galvanostatic charge-discharge curves of the supercapacitor with Nafion electrolyte and Norit A Supra Eur carbon (NSEuNaf. Measured SA = 1500 m^2 g^{-1}). Current: ± 5 and ± 10 mA cm^{-2} (Lufrano and Staiti, 2004)

Figure 3.17 presents a typical potential-time plot obtained during galvanostatic charge-discharge curves for EDLC. The shape of the curve is linear in the potential range studied, proving the absence of Faradaic reactions. Faradaic reactions are the charge transferred across the electric field interface as a result of an electrochemical reaction. The capacitance of the cell was calculated from the slope of the ***E = f (t)*** curves using equation below:

$$C = \frac{I}{dV/dt} \tag{3.10}$$

where C is the capacitance of the EDLC in farad (F), *I* the discharge current in ampere (A) and *dV*/*dt* is the slope in volt per seconds (V s^{-1}).

The specific capacitance in farad per gram (F g^{-1}) was calculated using the equation below [Xue *et al.*, 2008]:

$$C_m = \frac{C}{m} = \frac{Q}{m\Delta V} = \frac{I\Delta t}{m\Delta V} \tag{3.11}$$

where C_m is the specific capacitance (F g^{-1}), m is the electrode mass, I is the constant charge-discharge current (A), Δt is the time of discharge (s) and ΔV is the range of charge-discharge (V).

The stored energy, E is given by the simple formula [Yang *et al.*, 2005]:

$$E = \frac{1}{2} CV^2 \tag{3.12}$$

Power delivered from EDLC was calculated using equation below [Staiti *et al.*, 2002]:

$$P = \frac{V^2}{4R} \tag{3.13}$$

where R is internal resistance in EDLC cell.

The efficiency, η was calculated using the equation:

$$\eta = \frac{t_d}{t_c} x100\% = \frac{C_d}{C_c} x100\ \% \tag{3.14}$$

where t_d and t_c are the times for galvanostatic discharging and charging respectively meanwhile C_d and C_c are discharging and charging capacitance respectively [Tripathi *et al*., 2006].

From voltage loss upon discharge, d.c. resistance can be estimated using the equation below:

$$R=\frac{V_{drop}}{i} \tag{3.15}$$

where V_{drop} is the IR_{drop} and i is the constant discharge current.

3.9 Summary

This chapter presents the preparation of MC based polymer electrolytes. All samples were characterized using X-ray diffraction (XRD), Fourier transform infrared (FTIR), thermogravimetric analysis (TGA) and electrochemical impedance spectroscopy (EIS). The highest conducting sample was used as membrane in electrical double layer capacitor (EDLC) and the EDLC preparation method have been introduced in this chapter.